

Electronic Supporting Information for:

# A New Lamellar Gold Thiolate Coordination Polymer, $[\text{Au}(m\text{-SPhCO}_2\text{H})]_n$ , for the Formation of Luminescent Polymer Composites

Oleksandra Veselska <sup>1</sup>, Nathalie Guillou <sup>2</sup>, Gilles Ledoux <sup>3</sup>, Chia-Ching Huang <sup>4</sup>, Katerina Dohnalova Newell <sup>4</sup>, Erik Elkaïm <sup>5</sup>, Alexandra Fateeva <sup>6</sup> and Aude Demessence <sup>1,\*</sup>

<sup>1</sup> Institut de Recherches sur la Catalyse et l'Environnement de Lyon (IRCELYON), Université Claude Bernard Lyon 1, UMR CNRS 5256, 69626 Villeurbanne, France; oleksandra.veselska@ircelyon.univ-lyon1.fr

<sup>2</sup> Institut Lavoisier de Versailles (ILV), UVSQ, Université Paris-Saclay, UMR CNRS 8180, 78035 Versailles, France; nathalie.guillou@uvsq.fr

<sup>3</sup> Institut Lumière Matière (ILM), Université Claude Bernard Lyon 1, UMR CNRS 5306, 69626 Villeurbanne, France; gilles.ledoux@univ-lyon1.fr

<sup>4</sup> Institute of Physics, University of Amsterdam, Science Park 904, 1098 XH Amsterdam, The Netherlands; c.huang@uva.nl (C.-C.H.); k.newell@uva.nl (K.D.N.)

<sup>5</sup> Beamline Cristal, Synchrotron Soleil, 91192 Gif-sur-Yvette, France; erik.elkaim@synchrotron-soleil.fr

<sup>6</sup> Laboratoire des Multimatériaux et Interfaces (LMI), Université Claude Bernard Lyon 1, UMR CNRS 5615, 69626 Villeurbanne, France; alexandra.fateeva@univ-lyon1.fr

\* Correspondence: aude.demessence@ircelyon.univ-lyon1.fr

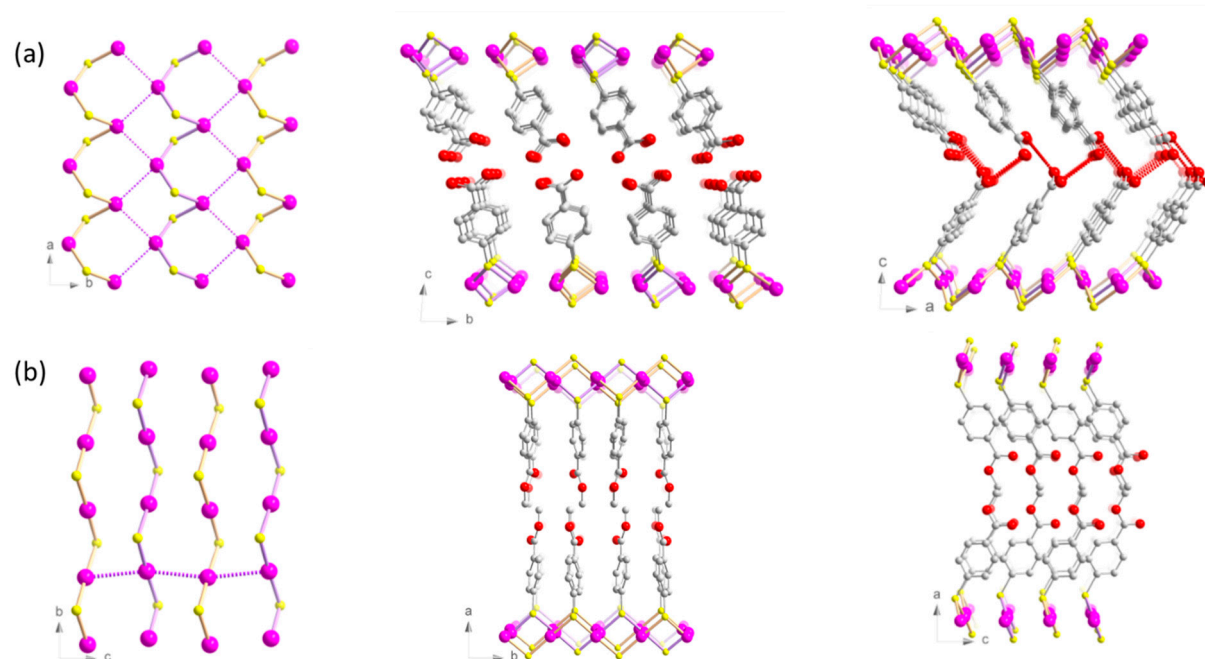


**Figure 1.** Structure representations of (a)  $[\text{Au}(p\text{-SPhCO}_2\text{H})]_n$  [1] and (b)  $[\text{Au}(p\text{-SPhCO}_2\text{Me})]_n$  [2]. Pink, Au; yellow, S; red, O; grey, C. Hydrogen atoms are omitted for clarity. Red and purple dotted lines represent the hydrogen bonds and the aurophilic interactions, respectively.

**Table S1** Crystallographic data and Rietveld refinement parameters for  $[\text{Au}(m\text{-SPhCO}_2\text{H})]_n$ .

Empirical formula	$\text{C}_7\text{H}_5\text{Au}_1\text{O}_2\text{S}_1$
$M_r$	350.15
Crystal system	Triclinic

Space group	<i>P1</i>
<i>a</i> (Å)	4.7567(5)
<i>b</i> (Å)	4.7632(6)
<i>c</i> (Å)	16.3975(5)
$\alpha$ (°)	90.780(8)
$\beta$ (°)	89.123(6)
$\gamma$ (°)	92.651(4)
<i>V</i> (Å <sup>3</sup> )	371.05(6)
<i>Z</i>	2
$\lambda$ (Å)	0.79276
Number of reflections	618
Number of fitted structural parameters	27
$R_p, R_{wp}$	0.061, 0.090
$R_{Bragg}, GoF$	0.037, 1.68

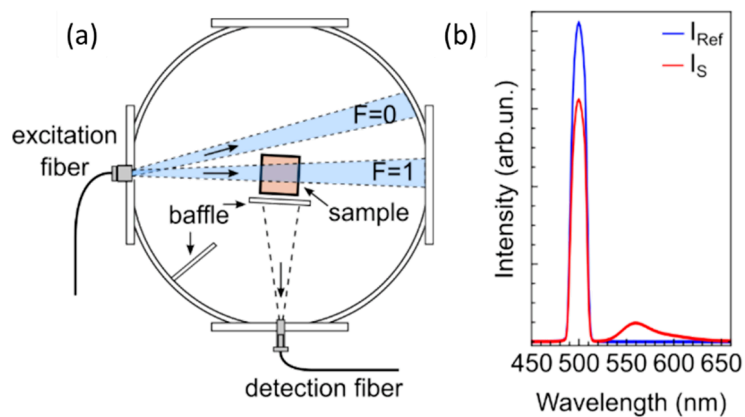


**Figure 2.** A scheme of a used standard integrating sphere setup was used (a) and a graphical representation of emission intensities detected with sample and reference (b).

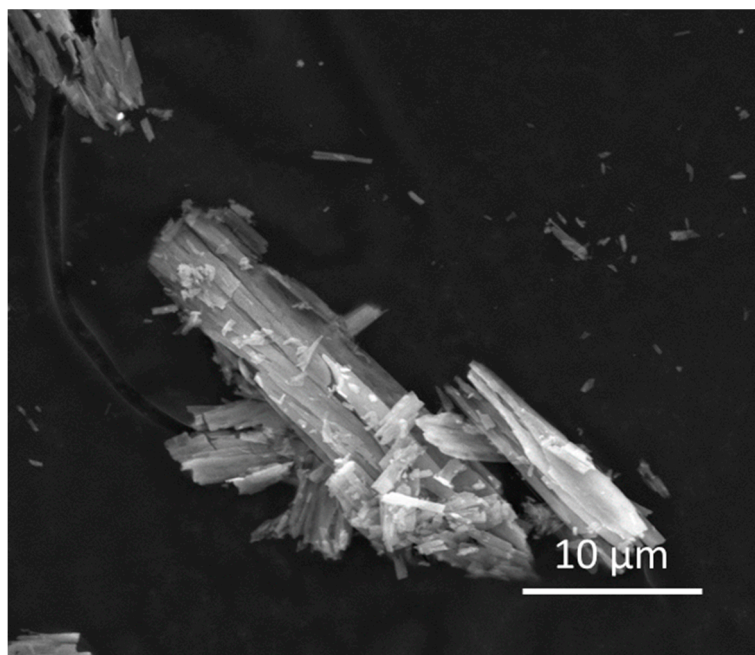


Figure 3. SEM image of [Au(*m*-SPhCO<sub>2</sub>H)]<sub>n</sub>.

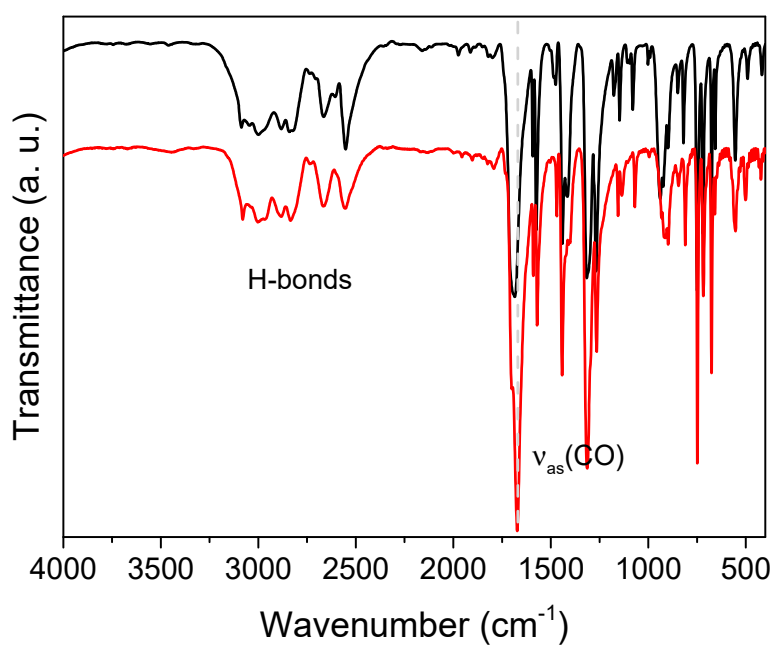


Figure 4. FT-IR spectra of the free ligand (black) and [Au(*m*-SPhCO<sub>2</sub>H)]<sub>n</sub> (red).

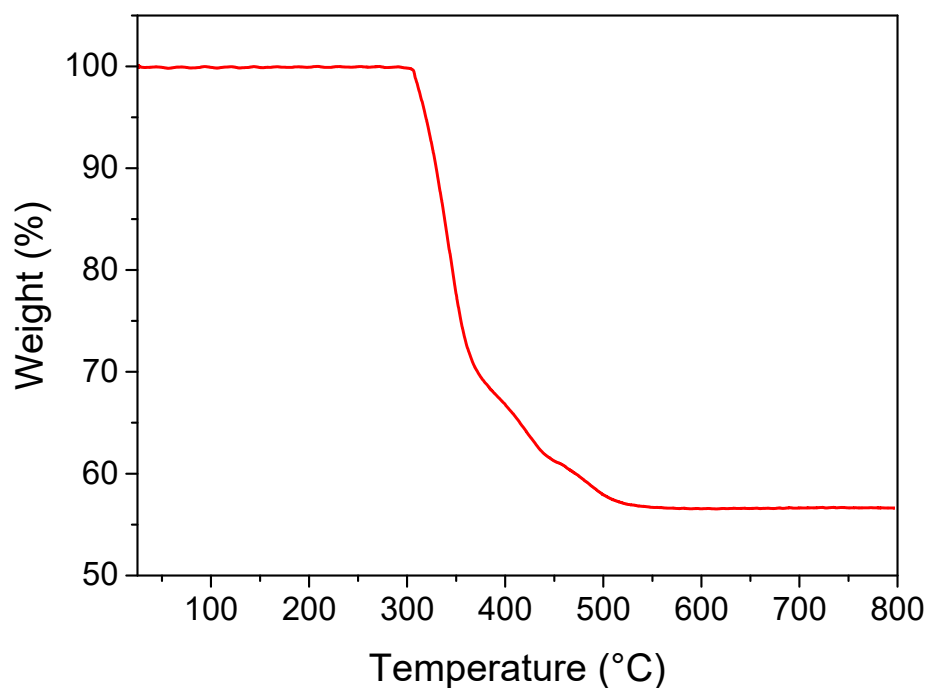


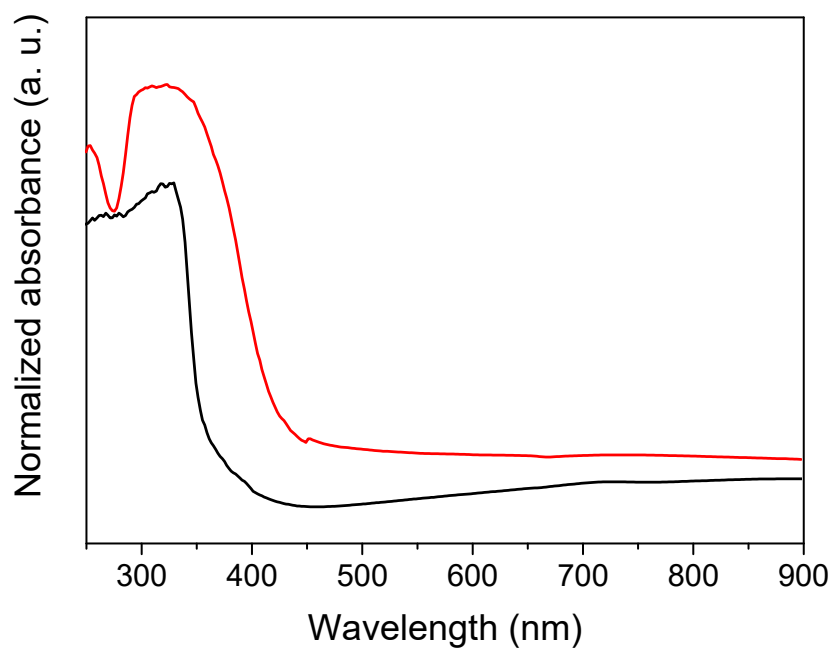
Figure 5. The TGA conducted under air at 10°C/min of [Au(*m*-SPhCO<sub>2</sub>H)]<sub>n</sub>.

Table 2. Comparison of the main distances and angles in [Au(*m*-SPhCO<sub>2</sub>H)]<sub>n</sub> and other lamellar [Au(SR)]<sub>n</sub> CPs, [Au(*p*-SPhCO<sub>2</sub>H)]<sub>n</sub> [1] and [Au(*p*-SPhCO<sub>2</sub>Me)]<sub>n</sub> [2].

Compound	Au-S Å	Au-Au Å	S-Au-S °	Au-S-Au °	O1-O2 Å	π-π Å	C-H... π Å
[Au( <i>m</i> -SPhCO <sub>2</sub> H)] <sub>n</sub>	2.28(2) 2.35(2) 2.36(2)	3.21(2)† 3.28(2)† 3.38(2)δ 3.61(2)δ	88.2(4) 151.1(5)	85.8(4) 90.5(4)	2.714(1) 3.039(1)	4.757(1)	
[Au( <i>p</i> -SPhCO <sub>2</sub> H)] <sub>n</sub>	2.27(1) 2.34(1) 2.37(1)	3.36(1)δ 3.42(1)δ 3.59(1)† 3.73(1)†	77.5(3) 124.0(4)	99.4(2) 110.4(2)	2.903(1) 3.011(1)	4.518(1)	
[Au( <i>p</i> -SPhCO <sub>2</sub> Me)] <sub>n</sub>	2.31(1)	3.20(1)δ 3.51(1)†	177.5(1)	97.1(1)	-	-	3.233(1) 4.200(1)

† Au-Au intrachain (bridged by sulfur atoms).

δ Au-Au interchain.



**Figure 6.** UV-vis absorption spectra of  $[\text{Au}(m\text{-SPhCO}_2\text{H})]_n$  (red) and the free ligand (black) conducted in solid state at the room temperature.

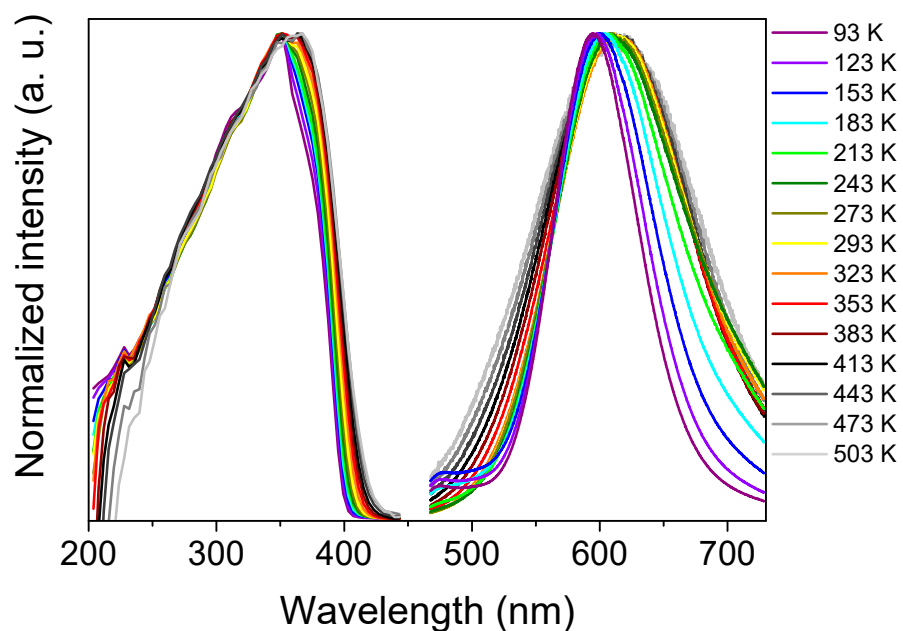


**Figure 7.** Normalized emission-excitation spectra ( $\lambda_{\text{exc}} = 352 \text{ nm}$ ,  $\lambda_{\text{em}} = 596 \text{ nm}$ ) of  $[\text{Au}(m\text{-SPhCO}_2\text{H})]_n$  conducted in solid state at variable temperatures.

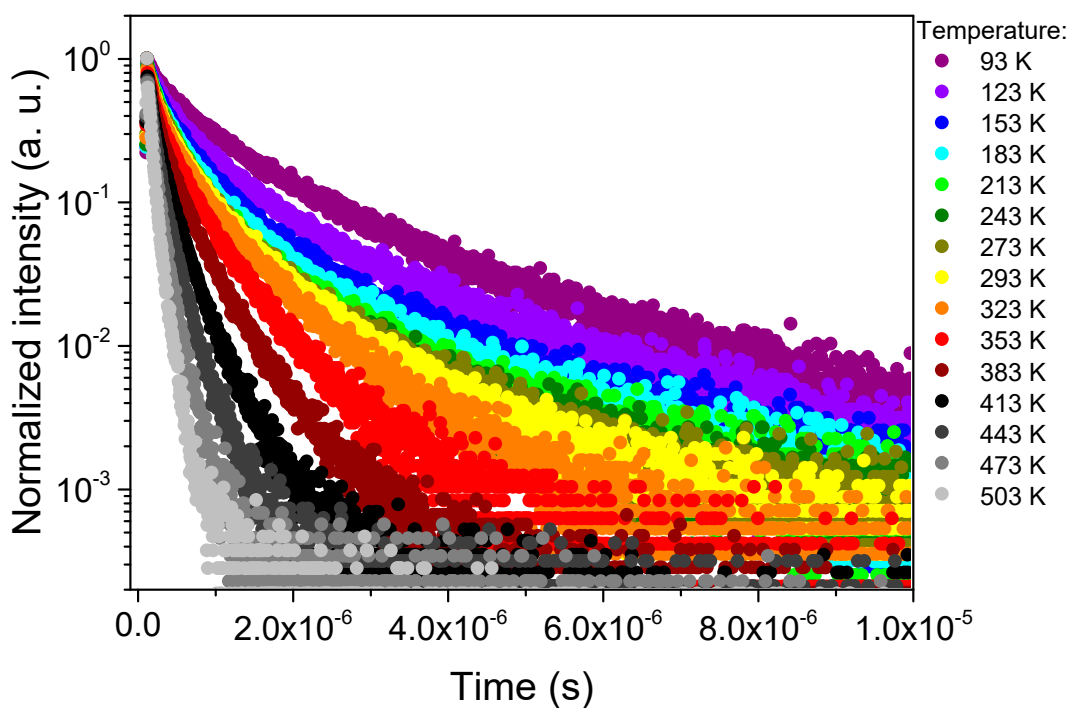


**Figure 8.** Temperature-dependent luminescence decay curves ( $\lambda_{\text{exc}} = 352 \text{ nm}$ ,  $\lambda_{\text{em}} = 610 \text{ nm}$ ) of  $[\text{Au}(m\text{-SPhCO}_2\text{H})]_n$  conducted in solid state at variable temperatures.

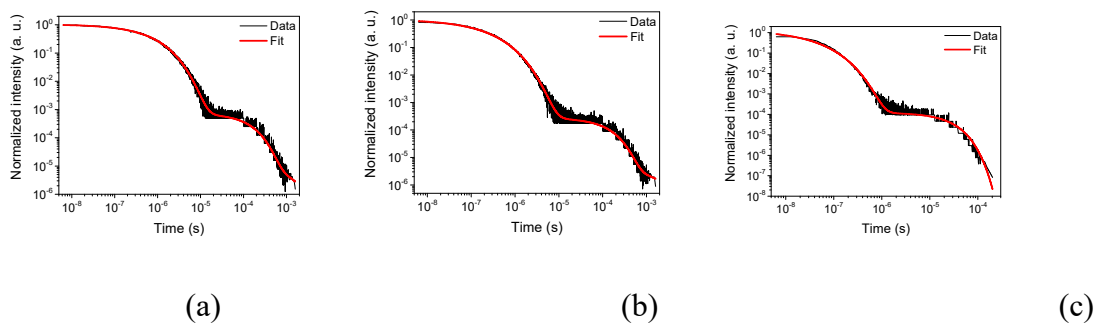
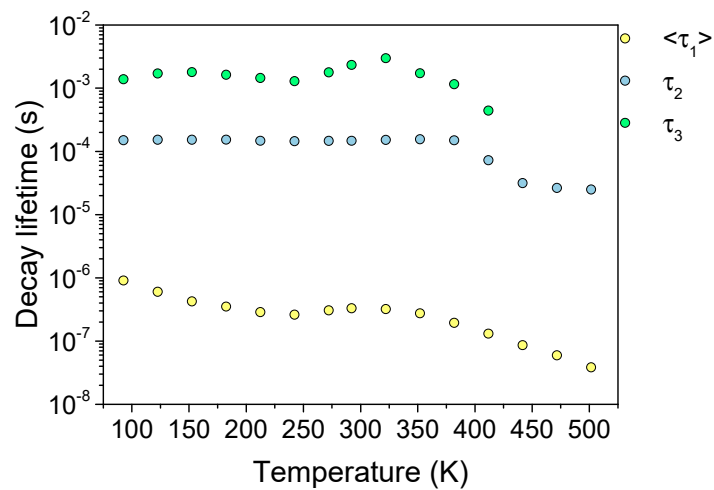
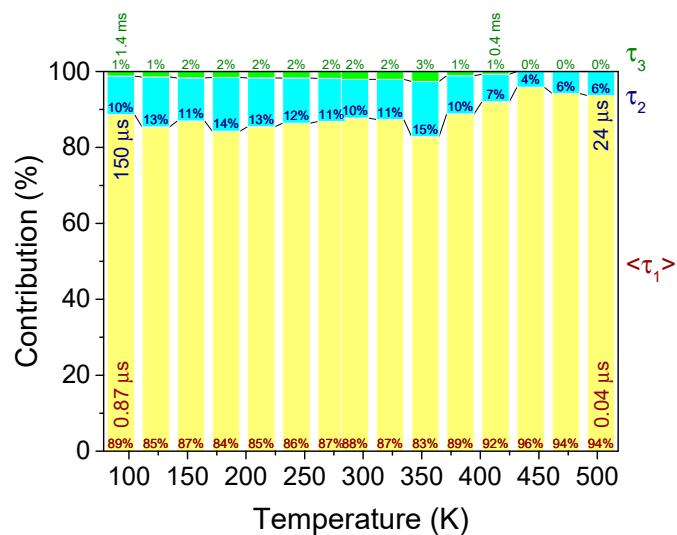


**Figure 9.** Examples of lifetime decay fit of  $[\text{Au}(m\text{-SPhCO}_2\text{H})]_n$  at 93 K (a), 293 K (b) and 503 K (c).



(a).



(b)

**Figure 10.** Temperature-dependent luminescence decays of  $[\text{Au}(m\text{-SPhCO}_2\text{H})]_n$ : values of the lifetime (a) and contributions (b) of different components at various temperatures.

Table S2 Luminescence lifetimes ( $\tau_i$ ), their pre-exponential factors ( $a_i$ ), parameters  $\beta_1$ , average lifetimes ( $\langle\tau_i\rangle$ ) and contributions of  $[\text{Au}(m\text{-SPhCO}_2\text{H})_n]$  at 93 to 503 K temperature range.

Temperature, K	$a_1 \pm \sigma a_1$	$\tau_1 \pm \sigma \tau_1, \text{ s}$	$\beta_1 \pm \sigma \beta_1$	$\langle\tau_1\rangle \pm \sigma\langle\tau_1\rangle, \text{ s}$	Contribution of $\tau_1, \%$	$a_2 \pm \sigma a_2$	$\tau_2 \pm \sigma \tau_2, \text{ s}$	Contribution of $\tau_2, \%$	$a_3 \pm \sigma a_3$	$\tau_3 \pm \sigma \tau_3, \text{ s}$	Contribution of $\tau_3 \%$	$R^2$
93	1.0281 ± 0.0058	6.35E-07 ± 6.96E-09	0.649 ± 0.003	8.69E-07 ± 1.01E-08	89	6.84E-04 ± 4.39E-06	1.47E-04 ± 8.62E-07	10	8.93E-06 ± 5.37E-07	1.37E-03 ± 8.70E-05	1	0.99775
123	1.0663 ± 0.0070	3.67E-07 ± 4.80E-09	0.583 ± 0.002	5.74E-07 ± 7.92E-09	85	6.20E-04 ± 3.78E-06	1.49E-04 ± 8.06E-07	13	5.95E-06 ± 3.90E-07	1.69E-03 ± 1.41E-04	1	0.99772
153	1.1449 ± 0.0093	2.26E-07 ± 3.65E-09	0.533 ± 0.002	4.05E-07 ± 6.86E-09	87	3.96E-04 ± 2.65E-06	1.49E-04 ± 9.46E-07	11	4.91E-06 ± 3.22E-07	1.77E-03 ± 1.57E-04	2	0.99741
183	1.1843 ± 0.0102	1.77E-07 ± 3.04E-09	0.516 ± 0.002	3.34E-07 ± 6.03E-09	84	4.32E-04 ± 2.72E-06	1.50E-04 ± 8.72E-07	14	4.42E-06 ± 3.10E-07	1.61E-03 ± 1.38E-04	2	0.99746
213	1.3044 ± 0.0128	1.33E-07 ± 2.59E-09	0.492 ± 0.002	2.74E-07 ± 5.63E-09	85	3.63E-04 ± 2.45E-06	1.44E-04 ± 9.28E-07	13	4.80E-06 ± 3.09E-07	1.43E-03 ± 1.03E-04	2	0.99724
243	1.3183 ± 0.0131	1.17E-07 ± 2.31E-09	0.484 ± 0.002	2.49E-07 ± 5.17E-09	86	3.09E-04 ± 2.08E-06	1.41E-04 ± 9.43E-07	12	5.05E-06 ± 2.98E-07	1.27E-03 ± 7.53E-05	2	0.99736
273	1.1665 ± 0.0105	1.57E-07 ± 2.75E-09	0.522 ± 0.002	2.91E-07 ± 5.33E-09	87	3.01E-04 ± 1.96E-06	1.43E-04 ± 9.05E-07	11	3.91E-06 ± 2.37E-07	1.76E-03 ± 1.47E-04	2	0.99738
293	1.0452 ± 0.0088	1.88E-07 ± 2.96E-09	0.556 ± 0.002	3.14E-07 ± 5.19E-09	88	2.57E-04 ± 1.65E-06	1.44E-04 ± 9.06E-07	10	3.30E-06 ± 1.93E-07	2.30E-03 ± 2.44E-04	2	0.99744
323	1.0032 ± 0.0074	2.02E-07 ± 2.68E-09	0.599 ± 0.002	3.04E-07 ± 4.23E-09	87	2.41E-04 ± 1.33E-06	1.49E-04 ± 8.01E-07	11	2.41E-06 ± 1.44E-07	2.95E-03 ± 4.02E-04	2	0.99787
353	0.9304 ± 0.0070	1.89E-07 ± 2.41E-09	0.644 ± 0.003	2.61E-07 ± 3.51E-09	83	2.71E-04 ± 1.37E-06	1.52E-04 ± 7.88E-07	15	2.53E-06 ± 1.79E-07	1.70E-03 ± 1.54E-04	3	0.99777
383	0.9701 ± 0.0085	1.30E-07 ± 1.84E-09	0.629 ± 0.003	1.85E-07 ± 2.74E-09	89	1.33E-04 ± 7.15E-07	1.47E-04 ± 8.76E-07	10	1.87E-06 ± 1.27E-07	1.14E-03 ± 6.76E-05	1	0.99766
413	1.0048 ± 0.0103	8.74E-08 ± 1.40E-09	0.629 ± 0.003	1.24E-07 ± 2.08E-09	92	1.32E-04 ± 7.97E-07	7.05E-05 ± 4.49E-07	7	2.03E-06 ± 1.43E-07	4.34E-04 ± 2.04E-05	1	0.9973
443	1.1003 ± 0.0218	5.47E-08 ± 1.63E-09	0.604 ± 0.005	8.16E-08 ± 2.54E-09	96	1.16E-04 ± 1.16E-06	3.06E-05 ± 1.32E-07	4				0.99124
473	1.1470 ± 0.0237	3.84E-08 ± 1.14E-09	0.612 ± 0.005	5.63E-08 ± 1.74E-09	94	1.37E-04 ± 1.16E-06	2.56E-05 ± 8.14E-08	6				0.99275
503	1.3674 ± 0.0333	2.26E-08 ± 7.77E-10	0.574 ± 0.005	3.61E-08 ± 1.29E-09	94	1.16E-04 ± 9.21E-07	2.42E-05 ± 6.98E-08	6				0.99328



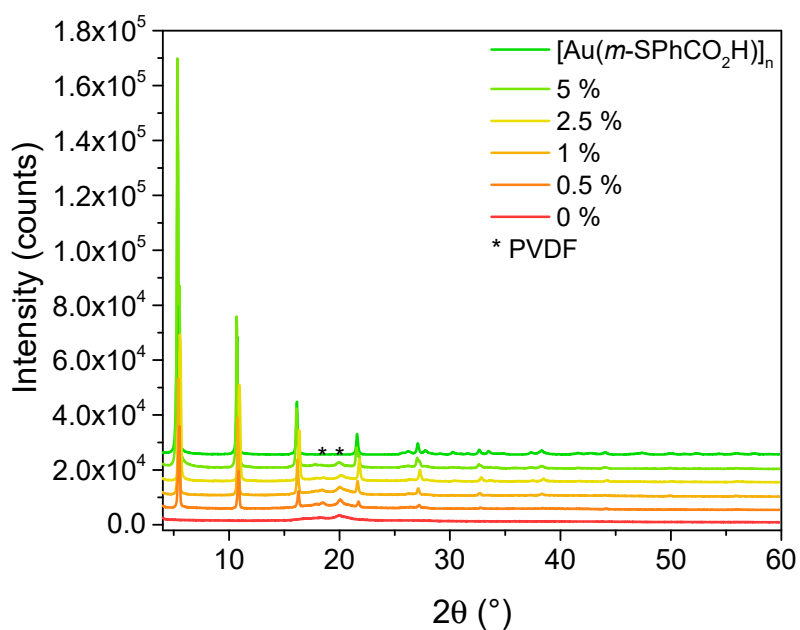


Figure 11. PXRD patterns of x % $[\text{Au}(m\text{-SPhCO}_2\text{H})]_n$ @PVDF films.

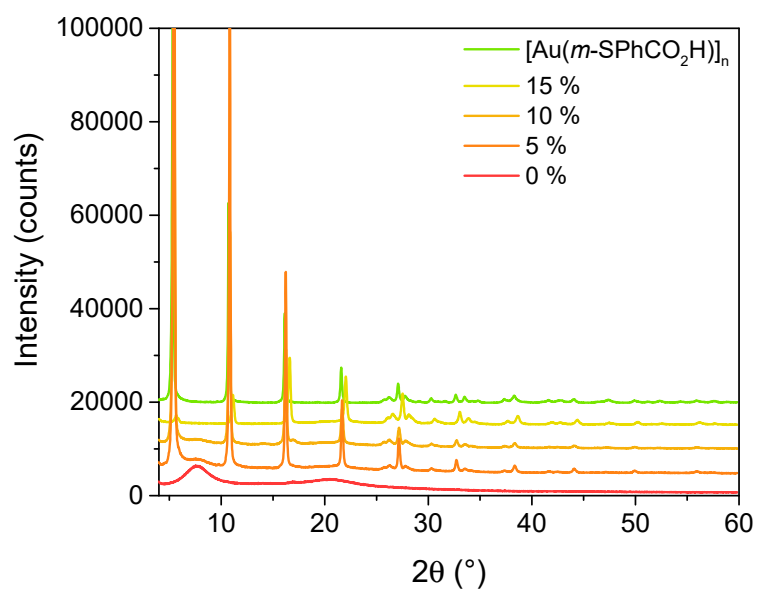


Figure 12. PXRD patterns of x % $[\text{Au}(m\text{-SPhCO}_2\text{H})]_n$ @PVK films.

## References

1. Veselska, O.; Okhrimenko, L.; Guillou, N.; Podbevšek, D.; Ledoux, G.; Dujardin, C.; Monge, M.; Chevrier, D. M.; Yang, R.; Zhang, P.; Fateeva, A.; Demessence, A., An intrinsic dual-emitting gold thiolate coordination polymer,  $[\text{Au}(+I)(p\text{-SPhCO}_2\text{H})]_n$ , for ratiometric temperature sensing. *J. Mater. Chem. C* **2017**, *5*, 9843.
2. Lavenn, C.; Guillou, N.; Monge, M.; Podbevšek, D.; Ledoux, G.; Fateeva, A.; Demessence, A., Shedding light on an ultra-bright photoluminescent lamellar gold thiolate coordination polymer  $[\text{Au}(p\text{-SPhCO}_2\text{Me})]_n$ . *Chem. Commun.* **2016**, *52*, 9063.